

Morphoacoustic perturbation analysis: principles and validation

Anthony Tew, Carl Hetherington, Jonathan Thorpe

▶ **To cite this version:**

Anthony Tew, Carl Hetherington, Jonathan Thorpe. Morphoacoustic perturbation analysis: principles and validation. Acoustics 2012, Apr 2012, Nantes, France. hal-00811131

HAL Id: hal-00811131
https://hal.science/hal-00811131

Submitted on 23 Apr 2012

HAL is a multi-disciplinary open access archive for the deposit and dissemination of scientific research documents, whether they are published or not. The documents may come from teaching and research institutions in France or abroad, or from public or private research centers.

L'archive ouverte pluridisciplinaire **HAL**, est destinée au dépôt et à la diffusion de documents scientifiques de niveau recherche, publiés ou non, émanant des établissements d'enseignement et de recherche français ou étrangers, des laboratoires publics ou privés.



ACOUSTICS 2012

Morphoacoustic perturbation analysis: principles and validation

A. I. Tew, C. T. Hetherington and J. B. Thorpe

University of York, Department of Electronics, Heslington, YO10 5DD York, UK
tony.tew@york.ac.uk

We present a frequency domain technique for investigating the relationship between acoustic properties of the human hearing system and the morphology responsible for creating them. Exploiting reciprocity, the boundary element method is applied to determine head-related transfer functions (HRTFs) for various directions and distances from a surface mesh model of a head and pinnae. Small orthogonal surface harmonic deformations are applied to the mesh one at a time and stored in a database together with the resulting, approximately linear, changes to the HRTFs (delta HRTFs). Once the computationally intensive process of constructing the database has been completed, identifying the morphological origins of arbitrary acoustic spectral features is very rapid. The method, which we term morphoacoustic perturbation analysis in the frequency domain (MPA-FD), is outlined and a proof-of-principle implementation described. MPA-FD is demonstrated by using it to determine the regions of the pinna responsible for determining the centre frequency of an HRTF notch and a peak. The predictions show good agreement with direct acoustic measurements.

1 Introduction

The acoustics of the human pinna have been studied for at least the last four decades [1,2]. The motivation to understand their role in sound localisation goes beyond scientific curiosity. They play a pivotal part in creating the acoustic spatial cues encapsulated in a head-related transfer function (HRTF). Since pinna shape is very individual, the spatial cues they produce are in general different for each listener. Spatial audio played through headphones needs to be tailored to account for this. Considerable effort is being directed towards making HRTF individualisation more effective and simpler to achieve. A promising route is to synthesise them based on knowledge of a listener's morphology. This paper describes a new technique for probing the relationship between human morphology and the HRTF acoustic features believed to carry spatial cues.

The steady increase in computing power has seen simple models for describing pinna function (e.g. [3]) superseded by increasingly sophisticated numerical analyses. Kahana and Nelson have conducted one of the most detailed and rigorous acoustical studies to-date on the pinna [4]. Using a high resolution mesh of KEMAR[1] they applied the boundary element method (BEM) up to 20 kHz to visualise acoustic modes supported by the pinna for a variety of source directions. They conclude that 'it is possible to implement individualised HRTFs in a 3-D sound system or an auditory display … if highly accurate 3-D images of the head and pinnae are captured and modelled with BEM.' Their work provides valuable insights into the pinna and has validated the use of the BEM for the acoustical analysis of the human hearing system.

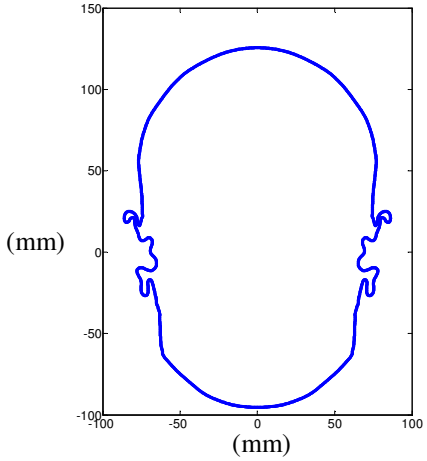


Figure 1: Contour generated by the P points in slice 1 of the KEMAR model.

[1] Knowles Electronic Manikin for Acoustics Research

More recently Mokhtari *et al.* [5,6] have reported the use of finite difference time domain methods to investigate the relationship between spectral features of HRTFs and the pinna regions responsible for creating them. By this means they have, for example, thrown new light on the mechanisms of pinna notch creation. Our technique, frequency domain morphoacoustic perturbation analysis (MPA-FD) has similar aims, but exhibits important differences in the way they are attained.

2 Principles of MPA-FD

2.1 The template head mesh

In the context of sound, we define morphoacoustics to be the study of relationships and interactions between the morphology (shape) of an object and its acoustic properties. Frequency domain morphoacoustic perturbation analysis (MPA-FD) involves the application of very small deformations to a closed mesh called the template which models the object under investigation. Only brief details are given here about how the mesh is produced. For the purposes of analysing the morphoacoustic properties of the human pinna, KEMAR's head and large pinnae were scanned and converted into a set of $S = 256$ slices. The left half-head was reflected in the median plane to replace the right half-head and each of the resulting symmetrical slice contours was uniformly sampled at $P = 2048$ points. Slice $s = 1$, lying in the vertical plane, is shown in Figure 1.

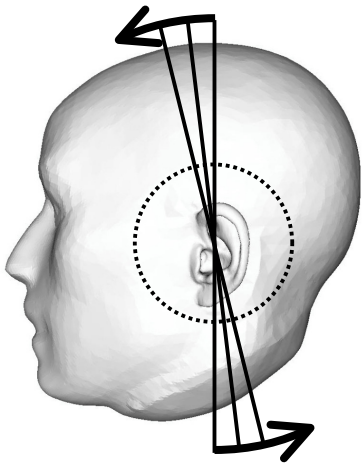


Figure 2: Template head radial slicing. Dotted line - an idealised cross-slice contour.

Slicing is performed radially around an axis through the two conchae (Figure 2) so that, with careful placement of the axis of rotation, the creation of disconnected secondary contours is avoided. A subset of the contour points was selected to become the nodes of the template mesh shown in the figure.

Head deformation is achieved by applying a small displacement $q_{s,p}$ ($0 \le s \le S-1$, $0 \le p \le P-1$) in the plane of the slice and locally perpendicular to the contour. The co-ordinates indexed by [*s*, *p*] can be flattened into a 2D, rectangularly bounded surface and the displacements analysed and synthesised using the 2D discrete Fourier transform.

$$q_{s,p} = \sum_{u=0}^{S-1}\sum_{v=0}^{P-1} Q_{u,v}\, e^{2\pi j\left(\frac{su}{S}+\frac{pv}{P}\right)} \tag{1}$$

u ($0 \le u \le S-1$) and v ($0 \le v \le P-1$) are the cross-slice (see Figure 2) and in-slice spatial harmonic numbers, respectively, and the associated surface harmonic coefficients $Q_{u,v}$ are given by

$$Q_{u,v} = \frac{1}{SP}\sum_{u=0}^{S-1}\sum_{v=0}^{P-1} q_{s,p}\, e^{-2\pi j\left(\frac{su}{S}+\frac{pv}{P}\right)} \tag{2}$$

where $q_{s,p}$ and $Q_{u,v}$ form a Fourier transform pair. Separating into real and imaginary parts, exploiting the Hermitian symmetry and making the substitutions

$$\begin{aligned} A_{u,v} &= Q_{u,v} + Q_{u,v}^{*} \\ &= 2\left|Q_{u,v}\right|\cos\angle Q_{u,v} \end{aligned} \tag{3}$$

and

$$\begin{aligned} B_{u,v} &= j\left(Q_{u,v} - Q_{u,v}^{*}\right) \\ &= -2\left|Q_{u,v}\right|\sin\angle Q_{u,v} \end{aligned} \tag{4}$$

Eq. (1) becomes

$$\begin{aligned} q_{s,p} = \sum_{u=0}^{S/2-1}\sum_{v=0}^{P/2-1}\Bigg\{ & A_{u,v}\cos\left[2\pi\left(\frac{su}{S}+\frac{pv}{P}\right)\right] \\ & + B_{u,v}\sin\left[2\pi\left(\frac{su}{S}+\frac{pv}{P}\right)\right]\Bigg\} \end{aligned} \tag{5}$$

The complete set of real-valued surface harmonic amplitude components may be written more compactly as

$$C_{u,v,\sigma} = \begin{cases} A_{u,v} & \text{for } \sigma = 0 \\ B_{u,v} & \text{for } \sigma = 1 \end{cases} \tag{6}$$

Given a sufficiently small set of displacements, and hence sufficiently small surface harmonic amplitudes, an arbitrary perturbation of the template will give rise to a linearly related change in acoustic pressure $\Delta p_{\theta,\phi,f}$ at the receiver. This leads to the total differential expression

$$\Delta p_{\theta,\phi,f} \approx \sum_{\sigma=0}^{1}\sum_{u=0}^{S/2-1}\sum_{v=0}^{P/2-1}\frac{\partial p_{\theta,\phi,f}}{\partial C_{u,v,\sigma}} C_{u,v,\sigma} \tag{7}$$

for $\left|q_{s,p}\right| \le q_{\max}$ for all *s* and *p*, where:

θ and ϕ are the azimuth and elevation, respectively, of a pressure source relative to the head and at a distance of 1 m;

f is the acoustic frequency;

$q_{\max}$ is the maximum displacement consistent with a substantially linear relationship between shape and pressure variation;

$\Delta p_{\theta,\phi,f}$ represents the change in pressure of an HRTF for a single frequency and direction as a result of introducing an arbitrary shape perturbation to the template. The set of such pressure changes over the discrete frequency range of interest is described by the vector $\mathbf{\Delta p}$, which can meaningfully be termed the delta HRTF (ΔHRTF).

$q_{\max}$ must be large enough to avoid contamination by computation noise and small enough for the morphological shape deformation to be acceptably linearly related to the resulting acoustic pressure changes. Based on a series of experiments, a value of 0.3 mm was initially chosen. (Subsequently, and after construction of the database, further studies suggest that a maximum contour displacement of 0.1 mm or less would lead to appreciably improved linearity and is still well above the noise floor).

2.2 Surface harmonic deformations

Surface harmonic deformations $c_{s,p,u,v,\sigma}$ with amplitude $q_{\max}$, for all combinations of *s*, *p*, *u*, *v* and σ, were applied individually to the MPA-FD template mesh (Figure 5):

$$c_{s,p,u,v,0} = q_{\max}\cos\left[2\pi\left(\frac{su}{S}+\frac{pv}{P}\right)\right] \tag{8}$$

$$c_{s,p,u,v,1} = q_{\max}\sin\left[2\pi\left(\frac{su}{S}+\frac{pv}{P}\right)\right] \tag{9}$$

Using reciprocity, the ΔHRTFs $\mathbf{\Delta p}_{\theta,\phi,\mathbf{u},\mathbf{v},\sigma}$ were calculated for several locations around the head in the frequency range 7.78 kHz to 12.22 kHz. The set of harmonic deformations and their associated ΔHRTFs constitute the MPA-FD database.

To keep down the computation time for generating the database, the number of polygons in the template mesh was made as small as possible. In the region of the pinna, the longest edge is approximately $\lambda/5.4$ at the maximum analysis frequency. Edge lengths generally violate the accepted limit of $\lambda/4$ over the rest of the head, necessitating a series of tests to validate the acoustic integrity of the mesh for its intended purpose.

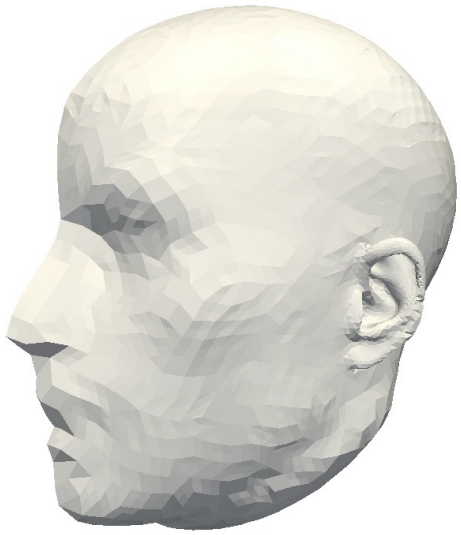
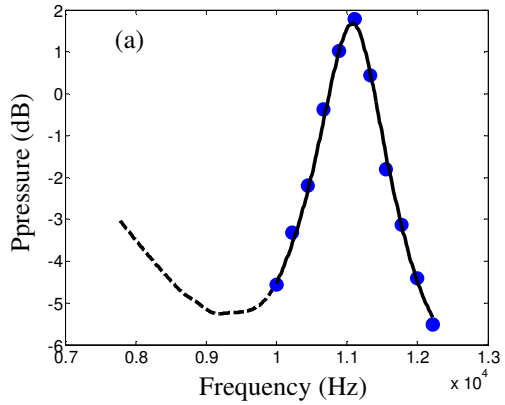


Figure 5: MPA-FD template mesh used for creating the database.

A simulated acoustic source was placed 6.4 mm from the occluded ear canal of the left ear. BEM simulations were conducted with this mesh and the resulting HRTFs compared with HRTFs created using a reference mesh which satisfied the λ/6 criterion in the pinna region and λ/4 elsewhere up to 15 kHz. Figure 6 (a) shows the reference and template HRTFs for the location 1 m directly above the head. Figure 6 (b) is a similar plot for the location 1 m behind the head. For the purposes of proof-of-principle testing it was considered acceptable for the template HRTFs to differ from the reference HRTFs by up to 1 dB or, near peaks and notches, for the centre frequencies to differ by up to 1%. For the directions investigated: directly in front, above, to the left, and behind; only one point (the highest frequency ringed in Fig. 6 (b)), exceeded these limits.

The database was populated with sine and cosine components for all combinations of cross-slice and in-slice harmonics up to and including $U = 20$ and $V = 30$. Increasing the number of coefficients improves the maximum resolution of the template deformations at the expense of increased computation time.



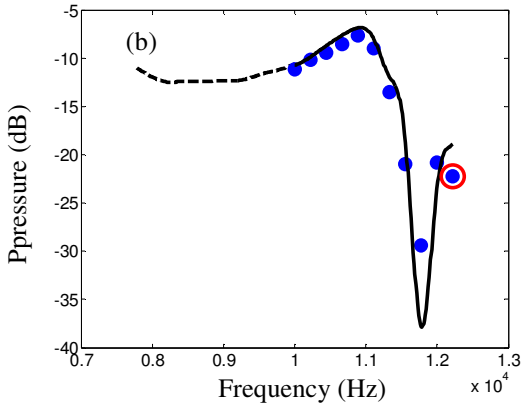


Figure 6: (a) HRTF for 1 m above the head. Line: HRTF for reference mesh; dots: HRTF for MPA-FD mesh. (b) HRTF for 1 m behind the head. The ringed point fails the similarity test

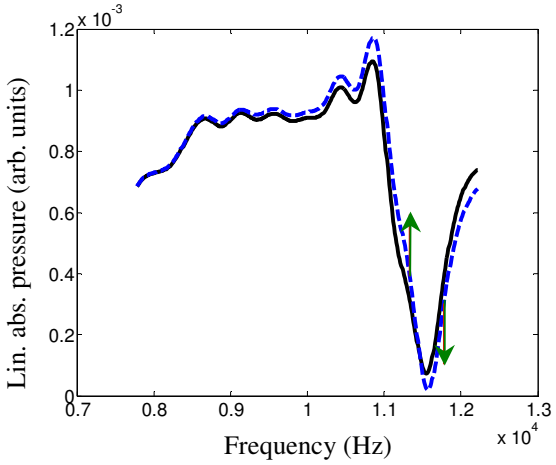


Figure 7: Line - original HRTF with notch. Dashes - HRTF plus weighted sum of ΔHRTF s. Arrows indicate morph vector values.

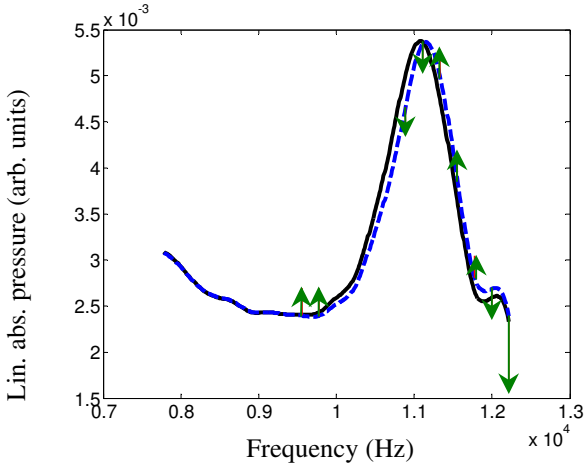


Figure 9: Line - original HRTF with peak. Dashes - HRTF plus weighted sum of ΔHRTF s. Arrows indicate morph vector values.

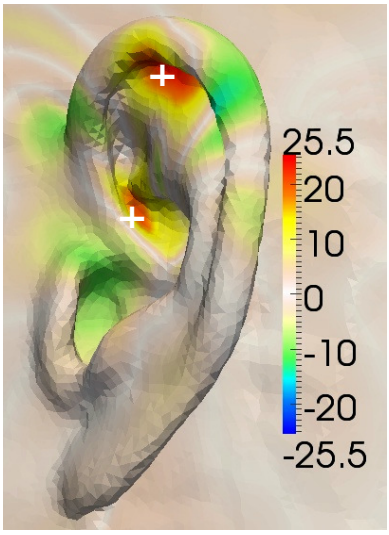


Figure 8: Red (+): morphology controlling notch frequency.

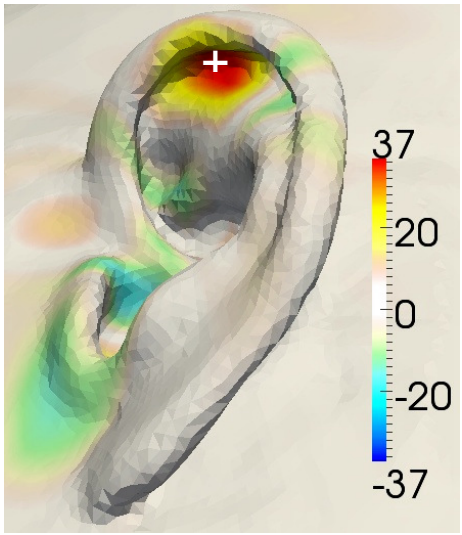


Figure 10: Red (+): morphology controlling peak frequency.

3 Application of MPA-FD

Once the database has been created, the acoustic effect of applying small perturbations to a mesh can be solved quickly. In the reverse direction it is possible to associate small changes in an HRTF with changes in morphology which will cause them. We demonstrate this by analysing two spectral features in an HRTF.

3.1 The morphological origin of a notch

The solid line in Figure 7 is the simulated HRTF for a location behind the template mesh (θ = -166°, ϕ = -2°). The dominant feature is a notch at approximately 11.5 kHz. An increase in centre frequency will cause the magnitude pressure to increase on the existing low frequency slope of the notch and decrease on the high frequency slope. The arrows in the figure indicate the scale and sense of the desired pressure changes. Scalar values in proportion to their length are assigned to morphing vector **m**. Forming the dot product of **m** with the ΔHRTF s $\mathbf{\Delta p}_{\theta,\phi,\mathbf{u},\mathbf{v},\sigma}$ in the database creates a set of weights *w*.

$$w_{\theta,\phi,u,v,\sigma} = \mathbf{m} \cdot \Delta \mathbf{p}_{\theta,\phi,u,v,\sigma} \tag{10}$$

The more closely a ΔHRTF in the database matches the morphing vector the greater the magnitude of its weight and the more it contributes to the desired pressure changes.

When the weighted ΔHRTF s are summed they result in an increase in the notch frequency, shown by the dashed line in Figure 7. The same weights are applied to the corresponding harmonic deformations in the database to create a scalar displacement μ of the template at each of its nodes.

$$\mu_{s,p} = \sum_{\sigma=0}^{1} \sum_{u=0}^{S/2-1} \sum_{v=0}^{P/2-1} w_{\theta,\phi,u,v,\sigma} c_{s,p,u,v,\sigma} \tag{11}$$

$|\mu|$ is greatest when harmonic deformations reinforce and this occurs in regions where the changes in pinna morphology most strongly affect the desired spectral change. In Figure 8 the surface of the mesh has been coloured according to the local value of μ. In this case there are two active regions and both have positive values of μ, indicating that a bulge in the surface here creates an upward shift in the frequency of the notch.

3.2 The morphological origin of a peak

A similar analysis is described for finding the regions of the pinna associated with the frequency of a peak. The HRTF (θ = 82°, ϕ = 76) above the head is shown in Figure 9. In this case the morphing vector **m** was adjusted until the peak was not only shifted up in frequency, but also maintained close to its original level, as shown in the figure. The implicated morphology is shown in Figure 10.

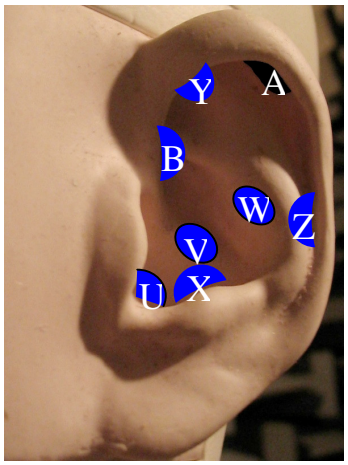


Figure 11: Putty sites used to validate notch analysis.

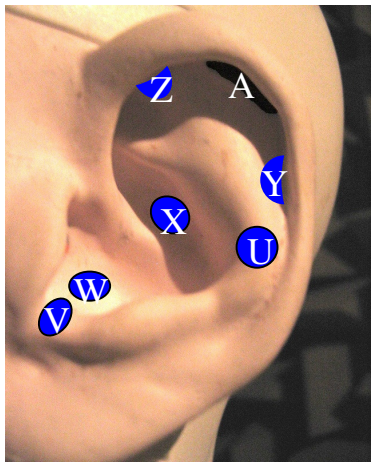


Figure 13: Putty sites used to validate peak analysis.

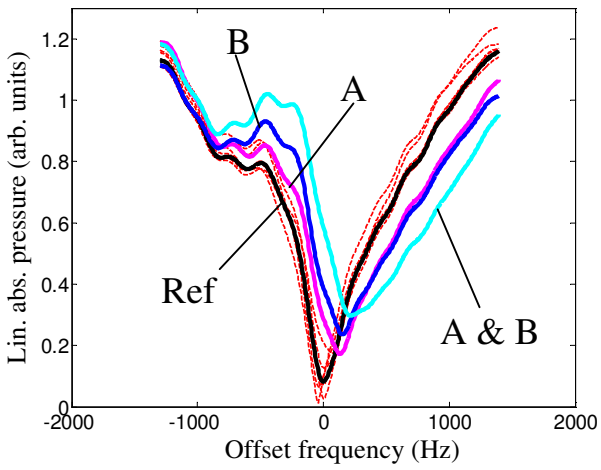


Figure 12: Ref - original HRTF. Putty in active regions A & B shifts notch more than putty at U to Z (dashed lines).

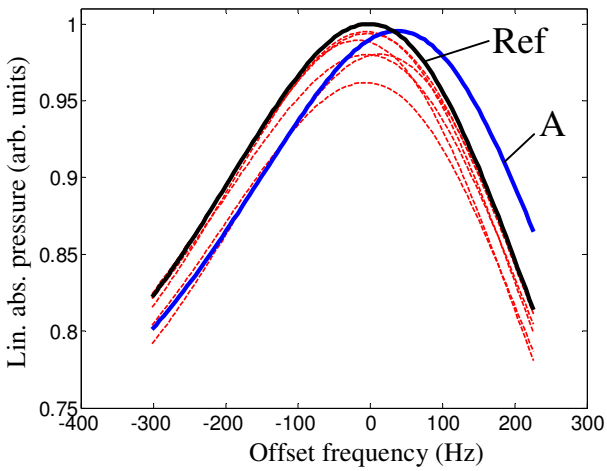


Figure 14: Ref - original HRTF. Putty at A shifts peak more than putty at U to Z (dashed lines).

4 Validation

Acoustic measurements in an anechoic chamber were conducted to confirm the validity of the predictions presented in Section 3. For the notch validation, about 22 mm^3 of putty was partially flattened, sculpted to the local shape of the pinna and attached at each of the sites shown in Figure 11. A and B are the regions chiefly implicated in determining the notch frequency; U to Z are arbitrary positions inside the pinna predicted to be less involved. Using a Sennheiser microphone, type KE 4-211-2, mounted so as to occlude the ear canal, HRTFs were measured with the putty in each position in turn.

The results in Figure 12 show that the notch frequency has indeed been raised more for putty in positions A and B. With the putty in each of the other positions the frequency shift is substantially smaller. When putty is applied simultaneously to positions A and B, the upward frequency shift is greater still, but there is an even greater loss of notch depth. A deep notch depends on very precise signal cancellation. For ease of handling, the putty slivers were several times thicker than $q_{\max}$ and will have driven the acoustic measurements beyond the linear region modelled in the database. This may have contributed to the deviation from the predicted response.

The implicated morphology for the HRTF peak was validated in a similar way and the results are shown in Figures 13 and 14. It is clear that only with the putty at the active site has the frequency of the peak increased substantially; furthermore, its level is substantially unchanged.

5 Discussion

MPA-FD has several appealing characteristics. The synthesis of morphologically active regions involves computing the dot products of the weight vector *w* with each harmonic displacement vector *c* and summing the result for each mesh node. This can be performed quickly with computation times potentially in the order of seconds. Furthermore, the resolution with which the active region is identified is dependent on the number of harmonics used. This provides a useful trade-off between speed and resolution.

New methods, such as FMBEM [8], for solving large problems with the BEM make a full analysis of the head and upper torso using MPA-FD a realistic prospect. In collaboration with PACSYS Ltd [7], work is underway to switch to an iterative solver, where the template BEM solution will act as a seed for solving each harmonic deformation, facilitating rapid convergence. Using reciprocity, the simulated source is situated adjacent to the occluded ear canal and once the pressures over the surface of the object have been calculated there is only a small additional computational cost in creating databases for a large number of HRTF directions.

6 Conclusion

A proof-of-principle implementation of a new technique known as morphoacoustic perturbation analysis in the frequency domain (MPA-FD) has been presented. Its ability to identify the morphological origin of an HRTF notch and peak has been demonstrated. MPA-FD is directly applicable to current efforts to derive HRTFs from morphology, for example by revealing those regions requiring careful measurement. Once the underlying surface harmonic database has been generated for a particular morphology, the computational load in performing each analysis is relatively low.

Acknowledgements

The authors are indebted to Dr Patrick Macey of PACSYS Ltd for his support of the PAFEC-FE BEM software and for his expert advice, to Aaron Turner and providers of the White Rose Grid parallel computing facility at York and to Andy Patterson for providing nightly access to the laboratory teaching computer network. This work was funded by EPSRC on grant GR/T28140/01.

References

[1] M. B. Gardner & R. S. Gardner, "Problem of Localization in the Median Plane: Effect of Pinna Cavity Occlusion," *J. Acoust. Soc. Am.* 53(2), 400-408 (1973)

[2] J. Hebrank & D. Wright, "Spectral cues used in the localization of sound sources on the median plane," *J. Acoust. Soc. Am.*, 56(6), 1829-1834 (1974)

[3] A. Lopez-Poveda & R. Meddis, "A physical model of sound diffraction and reflections in the human concha," *J. Acoust. Soc. Am.*, 100(5), 3248-3259 (1996)

[4] Y. Kahana & P. A. Nelson, "Boundary element simulations of the transfer function of human heads and baffled pinnae using accurate geometric models," *J. Sound & Vibration*, 300 (3-5), 552-579 (2007)

[5] P. Mokhtari, H. Takemoto, R. Nishimura & H. Kato, "Acoustic sensitivity to micro-perturbations of KEMAR's pinna surface geometry," *Proc. Int. Congress on Acoustics*, Sydney, Australia, 8 pp. (2010)

[6] P. Mokhtari, H. Takemoto, R. Nishimura & H. Kato, "Pinna sensitivity patterns reveal reflecting and diffracting surfaces that generate the first spectral notch in the front median plane," in *Proc. 36th IEEE Int. Conf. Acoust., Sp. and Sig. Proc. (ICASSP2011)*, Prague, Czech Republic 2408-2411 (2011)

[7] PAFEC-FE, PACSYS Ltd, http://www.pafec.co.uk/

[8] F. Nail, A. Gumerov, A. E. O'Donovan, R. Duraiswami & D. N. Zotkin, "Computation of the head-related transfer function via the fast multipole accelerated boundary element method and its spherical harmonic representation," *J.Acoust. Soc. Am.*, 127(1), 370-386 (2010)